IRS Deployment Under Practical Channel Model: Joint Position and Rotation Optimization

De Xu*, Tao Wang*, Nuocheng Yang*, Xinxin He*, Changchuan Yin*, Changsheng You†, and Haonan Tong‡
*Beijing Laboratory of Advanced Information Networks, Beijing University of Posts and Telecommunications, Beijing, China
†Department of Electrical and Electronic Engineering, Southern University of Science and Technology, Shenzhen, China
†Key Laboratory of Target Cognition and Application Technology (TCAT),
Aerospace Information Research Institute, Chinese Academy of Sciences, Beijing 100190, China
Emails:{xude, taowang, yangnuocheng, hxx_9000, ccyin}@bupt.edu.cn, youcs@sustech.edu.cn, tonghn@aircas.ac.cn

2025 11th International Conference on Computer and Communications (ICCC) | 979-8-3315-4558-1/25/$31.00 ©2025 IEEE | DOI: 10.1109/ICCC68654.2025.11437992

***Abstract*—In this paper, we study the deployment strategy of intelligent reflecting surfaces (IRS) for coverage extension, where the IRS is used to establish a cascaded link between the access point and users. Existing works have mostly adopted simplified channel models that consider only propagation path loss, overlooking critical IRS reception and reflection factors. To address this issue, we propose a practical channel model where the reception and reflection factors are explicitly derived based on electromagnetic field theory. Based on this channel model, we formulate an average achievable rate maximization problem over multiple users by jointly optimizing the position and rotation of the IRS. Due to the high-dimensional and coupled variable space of the formulated problem, we adopt a particle swarm optimization (PSO)-based algorithm, which efficiently obtains a near-optimal solution with significantly reduced computational complexity compared to exhaustive search. Numerical results demonstrate that our proposed scheme improves the achievable rate by at least 34.2% compared to conventional deployment strategies.**

***Index Terms*—IRS, deployment, position and location, channel model, particle swarm optimization (PSO).**

I. Introduction

Researchers are actively advancing sixth-generation (6G) wireless networks to achieve ultra-high data rates, improved energy efficiency, and broader coverage [1], enabling applications such as mixed reality, digital twins, and the Internet of Everything (IoE) [2]. While massive MIMO and relay systems enhance spectral and power efficiency, they incur high hardware and energy costs [3]. To address these challenges, intelligent reflecting surfaces (IRS) have emerged as a cost-effective and energy-efficient solution for coverage extension and capacity enhancement.

IRSs consist of numerous passive reflective elements in a planar array, each independently controlling the amplitude or phase of incident signals to enable adaptive reflection [4]. In particular, for coverage extension scenarios, where the-line-of sight (LoS) path from the access point (AP) to the target area is blocked, IRS can be properly deployed to bypass the obstacle and create a cascade virtual LoS link between transceiver [5].

In recent years, the IRS deployment strategy for coverage extension has been investigated in works [6]–[8]. Specifically, the authors in [6] analyzed IRS deployment at the AP side, user side, and both sides. They showed that user-side IRS works like active relays to enhance local coverage, while AP-side IRS provides higher beamforming gain and wider coverage. Moreover, they proposed a hybrid deployment combining both sides to exploit double-reflection links for improved system performance. Furthermore, in the dual distributed-IRS scenario, the authors in [7] enhanced coverage robustness by designing the element allocation and passive beamforming strategies for the two distributed IRSs where a two-step algorithm was adopted to maximize the worst-case signal-to-noise ratio (SNR) within the target area. The authors in [8] considered a multi-IRS-assisted communication system, optimizing both the IRS-UE association and IRS deployment locations to maximize ergodic capacity. Despite the effectiveness of the aforementioned IRS deployment strategies [6]–[8], they primarily adopted simplified channel models focusing only on propagation path loss, idealizing critical parameters such as the effective reception area, as well as the reception and reflection factors of IRS elements. These parameters fundamentally influence the accuracy of the IRS channel model and therefore need to be accurately modeled. Consequently, deployment strategies derived from such idealized models may suffer significant performance degradation in practical scenarios.

To address the above limitations, several recent studies have introduced more comprehensive IRS channel models [9]–[11]. Specifically, by explicitly incorporating the effective reception area, the authors in [9] jointly optimized the orientation and location of the IRS to maximize coverage, deriving a closed-form optimal orientation solution under the simplified assumption of ideal omnidirectional reception and reflection factors. Furthermore, the authors in [11] investigated IRS deployment strategies by approximating reception and reflection factors using the cosine approximation model [12], [13]. However, such approximations inherently oversimplify electromagnetic interactions, inevitably leading to suboptimal IRS deployment solutions in realistic scenarios.

To address the limitations mentioned above, we propose an IRS deployment strategy based on a practical channel model explicitly derived from electromagnetic field theory. The main contributions of this paper are summarized as follows:

- We propose a practical channel model based on electromagnetic field modeling. Based on the channel model, we formulate an optimization problem in a multi-user

This work was supported by the National Natural Science Foundation of China under Grant 62471056, Beijing Natural Science Foundation under Grant L223027 and L242084, and in part by the China 973 Program under Grant 2009CB320407.

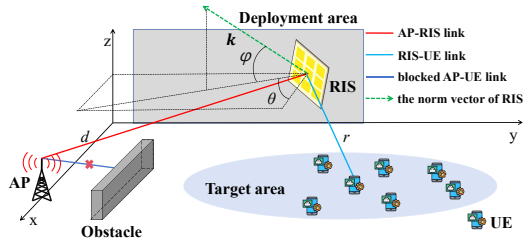

Fig. 1. A IRS-assisted wireless system for coverage extension, where the location and the rotation angle of the IRS need to be optimized.

scenario to maximize the average achievable rate of the IRS-assisted communication system by jointly optimizing the position and rotation of the IRS.

- To solve the formulated problem, we propose a particle swarm optimization (PSO)-based IRS deployment strategy for coverage extension. The proposed algorithm directly considers the average performance over all users in the target area and is further tailored for IRS orientation adjustment during the operation phase after IRS deployment, which has an extremely low computational complexity.
- Numerical results demonstrate that our scheme significantly enhances the average achievable rate compared to existing deployment strategies. Furthermore, the proposed method can also effectively deal with the change of target area during operation.

Notations: In this paper, scalars are denoted by non-bold italics letters, vectors by bold-face lower-case letters, and matrices by bold-face upper-case letters. The floor(x) represents the largest integer not greater than x. The mod(a, b) returns the remainder after division of a by b. For a vector $\boldsymbol{x}$, $\|\boldsymbol{x}\|$, $\boldsymbol{x}^T$, $\boldsymbol{x}^H$ and $[\boldsymbol{x}]_m$ denotes its Euclidean norm, transpose, conjugate transpose and m-th element, respectively. The diag$(\boldsymbol{x})$ forms a diagonal matrix with $\boldsymbol{x}$'s elements on the diagonal. j denotes the imaginary unit, i.e., $j^2 = -1$.

II. System Model

As shown in Fig. 1, we consider an IRS-assisted downlink wireless communication system consisting of a single-antenna AP and an IRS, where single-antenna UEs are located within the target area. The IRS is composed of N^{r} rows and N^{c} columns, i.e., totally $M = N^{\mathrm{r}} \times N^{\mathrm{c}}$ elements. Without loss of generality, the IRS center is placed on the y-z plane of the coordinate, with each IRS element having the size of $l \times l$.[1] We assume that there only exists the AP-IRS-UE link due to the obstacle, and both the AP and the UE are located in the far-field region of the IRS. For simplicity, we assume that there is no coupling between adjacent IRS elements during signal reflection. We focus only on signals that are reflected by the IRS once, ignoring those that undergo multiple reflections.

A. Practical Channel Model Accounting for Rotation of IRS

Conventional IRS deployment schemes assume that IRS is attached to the surface of the building, where its rotation angles are not adjustable. However, using stepper rotation machinery or simply fixed structures, the rotation angle of IRS is practically adjustable which proves to provide the IRS with an additional degree of freedom (DoF) to significantly enhance the performance of coverage extension [14]. Therefore, we consider the case of rotatable IRS. As illustrated in Figure. 1, we denote the normal vector of IRS as $\boldsymbol{k}$. θ and φ represent the azimuth and elevation angles of $\boldsymbol{k}$. The normal vector $\boldsymbol{k}$ of the IRS is represented as: $\boldsymbol{k} = (\cos\theta\cos\varphi, -\sin\theta\cos\varphi, \sin\varphi)^T$. The IRS elements are placed on lines along two orthogonal directions: $\boldsymbol{n}_1 = (\sin\theta, \cos\theta, 0)^T$ and $\boldsymbol{n}_2 = (-\cos\theta\sin\varphi, \sin\theta\sin\varphi, \cos\varphi)^T$.

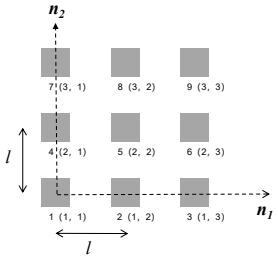

Fig. 2. An example of a 3x3 IRS, where each element of a specific row and a specific column is labeled with a unique index.

As illustrated in Fig. 2, to convey the coordinates of each element more intuitively, we map the N_m^{r}-th row and N_m^{c}-th column IRS element as the m-th IRS element, i.e., $N_m^{\mathrm{r}} = \mathrm{floor}(\frac{\mathrm{m}-1}{\mathrm{N^c}}) + 1$, $N_m^{\mathrm{c}} = m - N^{\mathrm{c}}(N_m^{\mathrm{r}} - 1)$. The center coordinates of the IRS is denoted by $\boldsymbol{p}_{\mathrm{c}} = [0, y, z]^T$ and the coordinates for the m-th element can be given by

$$\boldsymbol{p}_m = (N_m^{\mathrm{c}} - \frac{N^{\mathrm{c}}+1}{2})l\boldsymbol{n}_1 + (N_m^{\mathrm{r}} - \frac{N^{\mathrm{r}}+1}{2})l\boldsymbol{n}_2 + \boldsymbol{p}_{\mathrm{c}}. \quad (1)$$

Let $\boldsymbol{p}_{\mathrm{a}}$ and $\boldsymbol{p}_{\mathrm{u}}$ be the coordinates of AP and UE, respectively. The distance between the AP and the m-th IRS element is d_m, and the distance between the UE and the m-th IRS element is r_m, given by

$$d_m = \|\boldsymbol{p}_{\mathrm{a}} - \boldsymbol{p}_m\|, r_m = \|\boldsymbol{p}_{\mathrm{u}} - \boldsymbol{p}_m\|. \quad (2)$$

Similarly, the distance between the AP and the center of IRS is d, and the distance between the UE and the center of IRS is r, given by

$$d = \|\boldsymbol{p}_{\mathrm{a}} - \boldsymbol{p}_{\mathrm{c}}\|, r = \|\boldsymbol{p}_{\mathrm{u}} - \boldsymbol{p}_{\mathrm{c}}\|. \quad (3)$$

The LoS channels of AP-IRS link and IRS-UE link are denoted by $\boldsymbol{f} \in \mathbb{C}^{M\times 1}$ and $\boldsymbol{h}^H \in \mathbb{C}^{1\times M}$, respectively, which are given by[2]

$$[\boldsymbol{f}]_m = \sqrt{\frac{G_{\mathrm{a}}}{4\pi d_m^2}} e^{-\frac{j2\pi d_m}{\lambda}}, \quad (4)$$

$$[\boldsymbol{h}^{\mathrm{H}}]_m = \sqrt{\frac{G_{\mathrm{u}}}{4\pi r_m^2}\frac{\lambda^2}{4\pi}} e^{-\frac{j2\pi r_m}{\lambda}}, \quad (5)$$

[1] Square IRS element is adopted in this paper without loss of generality.

[2] The typical point, e.g., the center point, of the target area is regarded as the location of the potential UE, which is a common approach to address the deployment issues.

where $\frac{\lambda^2}{4\pi}$ represents the effective aperture of the UE antenna, G_{a} and G_{u} are the transmit gain of the AP antenna and the receiving gain of the UE antenna, respectively.

Lemma: The coefficient matrix $\mathbf{\Phi} \triangleq \mathrm{diag}(\beta_1, \cdots, \beta_M)$ introduced by the IRS can be given by [15]

$$\beta_m = \sqrt{\frac{4\pi l^4}{\lambda^2}} \cos\theta_m^i Z_m \mathrm{sinc}(X_m)\mathrm{sinc}(Y_m) e^{j\varphi_m}, \quad (6)$$

where X_m, Y_m and Z_m are intermediate variables, given by :

$$X_m = \frac{l}{\lambda} \sin\theta_m^r \cos\phi_m^r, \quad (7)$$

$$Y_m = \frac{l}{\lambda} (\sin\theta_m^r \sin\phi_m^r - \sin\theta_m^i), \quad (8)$$

$$Z_m = \sqrt{\sin^2\phi_m^r + \cos^2\theta_m^r \cos^2\phi_m^r}. \quad (9)$$

We use $\alpha_m \triangleq \cos\theta_m^i$ and $\gamma_m \triangleq Z_m \mathrm{sinc}(X_m)\mathrm{sinc}(Y_m)$ to denote the reception factor and the reflection factor of the m-th element. For the m-th element, θ_m^i, φ_m, θ_m^r and ϕ_m^r represent the incident angle, phase shift, and the elevation angle and azimuth angle of the reflected wave relative to the IRS plane, respectively, as illustrated in Fig. 7.

Proof. See Appendix A. □

The received signal at the UE can be given by

$$y = \boldsymbol{h}^{\mathrm{H}} \mathbf{\Phi} \boldsymbol{f} s + z, \quad (10)$$

where s denotes the symbol transmitted from AP with power P_{t}, $z \sim \mathcal{CN}(0, \sigma^2)$ denotes the received additive Gaussian white noise (AWGN) and σ^2 represents the noise power at the receiver. Substituting (4), (5), (6) into (10) yields the received signal power of UE, which is given by

$$P_{\mathrm{r}} = \frac{P_{\mathrm{t}} G_{\mathrm{a}} G_{\mathrm{u}} l^4}{16\pi^2} \left| \sum_{m=1}^{M} \frac{\alpha_m \gamma_m}{d_m r_m} e^{j\left(\varphi_m - \frac{2\pi}{\lambda}(d_m + r_m)\right)} \right|^2. \quad (11)$$

To maximize P_{r} in (11), we need to align the phases of total M paths created by the M IRS elements, i.e.,

$$\varphi_m = \mathrm{mod}\left(\frac{2\pi}{\lambda}(d_m + r_m), 2\pi\right). \quad (12)$$

By substituting (12) into (11), we obtain the received power with the optimal phase configuration given by

$$P_{\mathrm{r}} = \frac{P_{\mathrm{t}} G_{\mathrm{a}} G_{\mathrm{u}} l^4}{16\pi^2} \left| \sum_{m=1}^{M} \frac{\alpha_m \gamma_m}{d_m r_m} \right|^2. \quad (13)$$

In this paper, we consider both the AP and UE are located in the far-field of the IRS, so we make several approximations [3]. Next, the approximate received power is given by

$$P_{\mathrm{r}} = \frac{P_{\mathrm{t}} G_{\mathrm{a}} G_{\mathrm{u}} M^2 \alpha^2 \gamma^2 l^4}{16\pi^2 d^2 r^2}. \quad (14)$$

[3]We approximate $d_m \approx d$, $r_m \approx r$, $\theta_m^i \approx \theta_i$, $\theta_m^r \approx \theta_r$ and $\phi_m^r \approx \phi_r$, where θ_i, θ_r and ϕ_r are incident angle, the elevation and azimuth angles of the reflected wave of the center of IRS, respectively. Then, we obtain $\alpha_m \approx \alpha$, $\gamma_m \approx \gamma$. The approximations can only be applied in the calculation of channel amplitudes, but not for the channel phases since they are sensitive to the tiny variation (wavelength level change) of the distance [16].

From (14), we can see that by setting $\alpha = \gamma = 1$, the expression reduces to a form that neglects the reception and reflection factors, which is similar to the conventional cascaded path-loss models adopted in [4], [6], [16]. In contrast, our model explicitly incorporates these factors determined by the incident and reflection angles of the IRS which can substantially influence the received power and consequently the optimal IRS deployment. Notably, the incident and reflection angles are functions of the IRS rotation vector $\mathbf{\Omega} = (\theta, \varphi)^T$, meaning that $\mathbf{\Omega}$ directly affects α and γ and thus plays a critical role in the overall system performance.

The achievable rate at UE in bit/s/Hz (bps/Hz) is given by

$$R = \log_2(1 + \frac{P_{\mathrm{r}}}{\sigma^2}). \quad (15)$$

B. Problem Formulation

In practical communication systems, IRS need to be deployed in suitable areas for coverage extension. Let the IRS deployment position be denoted by $\boldsymbol{p}_{\mathrm{c}}$, and the set of candidate deployment positions be $\mathcal{S}$. The IRS orientation is determined by a rotation angle vector $\mathbf{\Omega}$, constrained by the set $\mathcal{A}$.

In the multi-user scenario, a time division multiplexing (TDM) strategy is considered, where the IRS position and orientation remain fixed during a scheduling cycle, and different users are served sequentially in separate time slots. Suppose there are K users in the area, with the position of the k-th user denoted by $\boldsymbol{u}_{\mathrm{k}}$, and its achievable rate by $R_k(\boldsymbol{p}_{\mathrm{c}}, \mathbf{\Omega})$. The optimization objective is to maximize the average achievable rate, formulated as

$$\max_{\boldsymbol{p}_{\mathrm{c}}, \mathbf{\Omega}} \quad \frac{1}{K} \sum_{k=1}^{K} R(\boldsymbol{p}_{\mathrm{c}}, \mathbf{\Omega}, \boldsymbol{u}_k) \quad (16)$$

$$\text{s.t.} \quad \boldsymbol{p}_{\mathrm{c}} \in \mathcal{S}, \quad (16a)$$

$$\mathbf{\Omega} \in \mathcal{A}. \quad (16b)$$

The problem in (16) is challenging to solve for the following reasons. As shown in (14), the parameters d, r, α, and γ are jointly determined by the optimization variables, which makes it difficult to obtain a closed-form solution through variable transformation techniques such as Lagrange duality. Moreover, since (14) is a non-convex function of the optimization variables, conventional convex optimization algorithms cannot be applied. To address this non-convex optimization problem, we adopt an efficient particle swarm optimization (PSO) algorithm.

III. Particle Swarm Optimization based IRS Deployment

Before determining the optimal deployment of the IRS, we first need to obtain the candidate locations and candidate rotation angles of the IRS based on the environmental information. Specifically, there are areas available for IRS deployment in the environment, e.g., the surrounding building surface. Within these areas, the candidate deployment areas should meet the following conditions: dominant LoS links exist from the AP to IRS and from IRS to the target area, so as to establish a virtual

Algorithm 1 PSO based IRS deployment

Input: Parameters for PSO: N, D, T, c_1, c_2, $W_{\max}$, $W_{\min}$.

Initialization: positions $\boldsymbol{u}$ and velocities $\boldsymbol{v}$ randomly within bounds, each particle's best position $\boldsymbol{p}$ and best fitness p_{best}, global best position $\boldsymbol{g}$ and best fitness g_{best}
for iteration $i = 1$ to T **do**
  for each particle $j = 1$ to N **do**
    if $R(\boldsymbol{u}(j)) > p_{\text{best}}(j)$ **then**
      $\boldsymbol{p}(j) \leftarrow \boldsymbol{u}(j)$ and $p_{\text{best}}(j) \leftarrow \boldsymbol{R}_{\mathbf{avg}}(\boldsymbol{u}(j))$
    end if
    if $p_{\text{best}}(j) > g_{\text{best}}$ **then**
      $\boldsymbol{g} \leftarrow \boldsymbol{p}(j)$ and $g_{\text{best}} \leftarrow p_{\text{best}}(j)$
    end if
    Calculate $w = W_{\max} - (W_{\max} - W_{\min}) \cdot i/T$
    Update $\boldsymbol{v}(j) \leftarrow w \cdot \boldsymbol{v}(j) + c_1 \cdot rand \cdot (\boldsymbol{p}(j) - \boldsymbol{u}(j)) + c_2 \cdot rand \cdot (\boldsymbol{g} - \boldsymbol{u}(j))$ and $\boldsymbol{u}(j) \leftarrow \boldsymbol{u}(j) + \boldsymbol{v}(j)$
  end for
end for

Output: $\boldsymbol{g}$ as the optimal solution

AP-IRS-UE LoS link that bypasses the obstacle. Besides, the candidate rotation angles of IRS should have the following conditions: both the AP and the target area are located within the reflective half-plane of the IRS. Based on meeting the above two conditions, the values of the candidate locations and rotation angles of IRS should be determined according to the specific environment settings. Without loss of generality, we set the candidate locations of IRS as $\mathcal{S} = \{(0, y, z)^T \mid y \in [0, 260], z \in [1, 110]\}$. The candidate rotation angles of IRS is set as $\mathcal{A} = \{(\theta, \varphi)^T \mid \theta \in [-90, 90], \varphi \in [-90, 90]\}$ in degree. Then, we apply the PSO algorithm to obtain the position and rotation angle configuration that yields the highest achievable rate selected as the optimal IRS deployment setting. Additionally, we apply an exhaustive search algorithm as a baseline for comparison in solving the proposed problem.

In the PSO algorithm, the parameters are set as follows: the particle count $N = 1000$, dimensionality $D = 4$, maximum iterations $T = 20$, and $rand$ representing a random number in the range $[0, 1]$. The cognitive and social coefficients are $c_1 = c_2 = 2$, balancing exploration and convergence. The inertia weight w varies linearly from $W_{\max} = 0.9$ to $W_{\min} = 0.4$ to enhance convergence stability. Position and velocity bounds are imposed to maintain feasible IRS deployments. In this paper, the position and velocity of each particle are defined as $\boldsymbol{u} = (y, z, \theta, \varphi)^T$ and $\boldsymbol{v} \in \mathbb{R}^{D\times 1}$. The range of values for the elements in $\boldsymbol{u}$ is consistent with sets $\mathcal{S}$ and $\mathcal{A}$, while the range of values for the elements in $\boldsymbol{v}$ is set within ±5. **Algorithm 1** shows the proposed IRS deployment strategy procedure. The computational complexity of the PSO algorithm is $O(NDT)$.

After the position of IRS is fixed, the IRS can respond to the change of the target area, e.g., the target area may change over time due to UE's movement, through adjusting its rotation angles. Note that this can be realized only when adjustable devices (e.g., stepper rotary machines) are equipped [17].

IV. Numerical Results

This section presents simulation results by considering the following setup unless otherwise specified. The channel model described in Section II is adopted, with parameters shown in Table I. We consider a target area centered at $\big(30, L, 0\big)$, where L is the y-coordinate of the area center and ranges

TABLE I
Parameter Configuration and Parameter Range

Parameters	Values	Parameters	Values
P_{t}	30 dBm	G_{u}	5
σ^2	-80 dBm	N^{r}	16
λ	0.125 m	N^{c}	16
l	0.0625 m	M	256
G_{a}	5 dB	$\boldsymbol{p}_{\text{a}}$	$(60, 0, 100)^T$

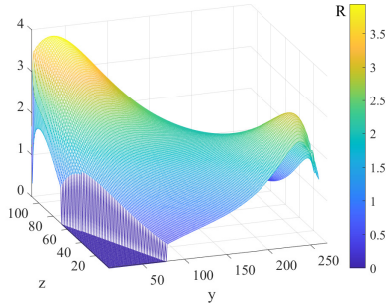

Fig. 3. Average achievable rate v.s. the IRS position with rotation angles fixed.

from 50 m to 250 m. For each L, $K = 20$ user locations are generated from a two-dimensional Gaussian distribution centered at $(30, L, 0)$. For comparison, we implement six schemes: 1) PSO scheme that obtains the optimal IRS position and angle configuration through the PSO algorithm; 2) exhaustive search scheme that obtains the optimal IRS position and angle configuration through the exhaustive search algorithm; 3) proposed model scheme that orientation of IRS is fixed based on the proposed channel model; 4) effective area scheme that considers the effective reception area of the IRS in deployment [9]; 5) cosine law scheme that the reception and reflection factors of IRS derived from a simplified cosine law approximation in deployment [11]; 6) conventional scheme that only considers the cascade path loss in deployment [16].

Fig. 3 shows the average achievable rate versus the IRS position. In this simulation, the IRS rotation angles are fixed at $\boldsymbol{\Omega} = (10, -10)^T$, and the average rate is computed for the given UE distribution described earlier. The resulting surface is both non-convex and truncated, due to the coupling of IRS position with multiple variables and the half-plane reflectivity of the IRS. This complexity makes identifying the optimal deployment position highly challenging, motivating the use of both the PSO algorithm and exhaustive search to obtain high-quality solutions.

Fig. 4 shows the average achievable rate versus the iteration number of the PSO algorithm. In the simulation, we evaluate the average achievable rate for the target area centered at $\boldsymbol{p}_{\text{u}} = (30, 250, 0)^T$ by the PSO algorithm. As shown in Fig. 4, the PSO algorithm converges by the sixth iteration, which is sufficient to demonstrate the high computation efficiency of the proposed algorithm for the IRS deployment.

Fig. 5 shows how the average achievable rate in the six schemes varies with the y coordinate of the target area center. As L increases, the average achievable rate gradually declines due to the increased path loss, which reduces the received power for users in the area. The cosine law scheme and the

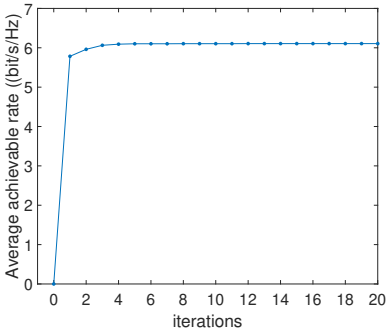

Fig. 4. Average achievable rate v.s. iteration Number of PSO algorithm

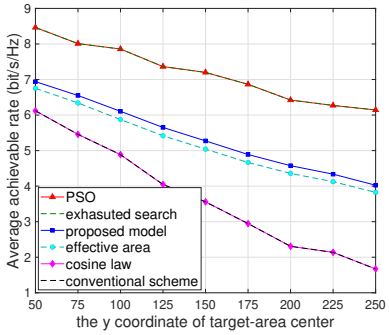

Fig. 5. Average achievable rate v.s. the y coordinate of target-area center.

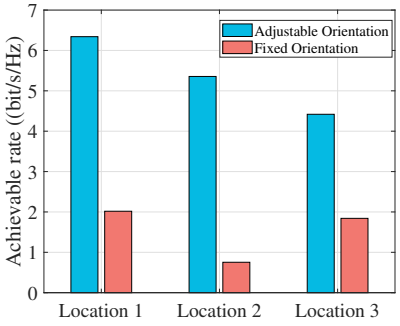

Fig. 6. Average achievable rate after IRS adjustment for different target areas.

TABLE II
THE VALUES OF RECEPTION FACTOR, REFLECTION FACTOR AND ACHIEVABLE RATE FOR DIFFERENT DEPLOYMENT SCHEMES

schemes	α	γ	$\alpha\gamma$	R
PSO	0.9114	0.9525	0.8681	6.6259
exhaustive search	0.9115	0.9495	0.8654	6.6255
proposed model	0.9223	0.8574	0.7907	4.5983
effective area	0.9844	0.7448	0.7332	4.3798
cosine law	0.2634	0.7361	0.1939	2.5885
conventional scheme	0.2634	0.7361	0.1939	2.5885

conventional scheme yield identical curves because maximizing the rate is equivalent to minimizing the cascaded path loss under the cosine law, resulting in the same deployment performance. The effective area scheme exhibits a slight drop compared to the proposed model scheme since it accounts only for the reception factor α. In contrast, the conventional scheme shows a substantial performance loss because it ignores both reception and reflection factors in the channel modeling, causing large deviations from the practical IRS channel. The PSO algorithm and exhaustive search achieve similar results, both offering significant improvements over baseline schemes, as the rotatable IRS effectively balances multiple factors to enhance the average achievable rate.

Table. II shows the reception factor α, reflection factor γ and achievable rate R for these six deployment schemes, where the values correspond to the case of a user located at the target area center ($L = 200$ m). From Table. II, it can be observed that the cosine law scheme and conventional scheme achieve the smallest product of α and γ, leading to the least achievable rate. Moreover, deployment strategies based on more practical models yield better performance, and IRS can significantly enhance the ability to balance multiple factors by considering more DoFs of IRS placement, i.e., the rotation angles, thus improving the system performance in terms of the achievable rate.

Fig. 6 shows the performance of the proposed scheme when the IRS's rotation angles are adjusted as the target area changes, illustrating the adaptability of our approach. In this simulation, we fix the IRS deployment location at $\boldsymbol{p}_c = (0, 99.6, 1)^T$, which is the optimal position when the target area center is at $(30, 100, 0)^T$. The other potential target area centers (Location 1, 2, and 3) are set as $(50, 80, 0)^T$, $(60, 50, 0)^T$, and $(80, 150, 0)^T$, respectively, with users randomly distributed around each center. As shown in Fig. 6, a fixed-orientation IRS suffers from reduced average achievable rate when the target area changes, due to lower reflection factors. In contrast, a rotatable IRS can flexibly adjust its orientation to match the new target area, effectively improving the average achievable rate.

In our experimental setup, the algorithms were executed on an Intel Core i5-12490F processor (base frequency 3.00 GHz), using the MATLAB platform. The PSO significantly reduced runtime from 83 minutes to 7 minutes and the adjustment step was completed in just 30 seconds, illustrating the high efficiency of our proposed algorithm.

V. CONCLUSION

In this paper, we propose a novel IRS deployment strategy to extend coverage for a target area. First, we consider a practical channel model based on electromagnetic field modeling and formulate an optimization problem to maximize the average achievable rate of the IRS-assisted communication system by jointly optimizing the IRS position and orientation. Next, we adopt a PSO algorithm to efficiently determine the optimal deployment configuration. Once the IRS is deployed, its orientation can be adaptively adjusted to accommodate changes in the target area. Numerical results show that the proposed algorithm efficiently and accurately finds near-optimal deployment strategies. Furthermore, the results indicate that our method significantly improves the average achievable rate and effectively adapts to target area changes during operation compared to conventional schemes.

APPENDIX A

Proof. We consider a perfectly conducting rectangular plate with dimensions $a \times b$ and negligible thickness, located in the x-y plane. A distant point source radiates linearly polarized waves with wave number $k = \frac{2\pi}{\lambda}$. For simplicity, we assume the electric field $\boldsymbol{E}_i$ is polarized along $\boldsymbol{e}_x$, while the magnetic field $\boldsymbol{H}_i$ lies in the y-z plane. The angle of incidence θ_i and the angle of reflection θ_r are defined as the angles between the Poynting vector and the plane's normal $\boldsymbol{e}_z$. Here, ϕ_r represents the azimuth angle of the scattered wave, while ψ denotes the angle between $\boldsymbol{r}$ and $\boldsymbol{r}'$, as illustrated in Fig. 7. The electric

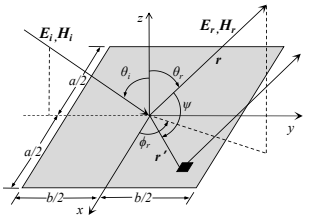

Fig. 7. The diagram of electromagnetic wave scattering by a metal plate.

and magnetic field components of the incident uniform plane wave can be written as:

$$\boldsymbol{E}_i = \boldsymbol{e}_x E_i e^{-jk(y\sin\theta_i - z\cos\theta_i)}, \tag{16}$$

$$\boldsymbol{H}_i = -\frac{E_i}{\eta}\left(\boldsymbol{e}_y\cos\theta_i + \boldsymbol{e}_z\sin\theta_i\right)e^{-jk(y\sin\theta_i - z\cos\theta_i)}, \tag{17}$$

where η is the characteristic impedance of the medium. Because the plate is a perfect electric conductor, its magnetization vector $\boldsymbol{M}_s = 0$. Given the negligible thickness of the surface, the induced surface current density can be approximated using physical optics given by

$$\boldsymbol{J}_s \approx 2\boldsymbol{e}_z \times \boldsymbol{H}_i|_{z=0, y=y'}. \tag{18}$$

Substituting (17) into (18), we obtain the following equation:

$$J_y = J_z = 0, J_x = \frac{2E_i}{\eta}\cos\theta_i e^{-jky'\sin\theta_i}. \tag{19}$$

We introduce two intermediate vectors $\boldsymbol{L}$ and $\boldsymbol{N}$ given by:

$$\boldsymbol{L} = \iint_S \boldsymbol{M}_s e^{jkr'\cos\psi}ds', \boldsymbol{N} = \iint_S \boldsymbol{J}_s e^{jkr'\cos\psi}ds'. \tag{20}$$

For ease of calculation, we use the rectangular-to-spherical component transformation:

$$\begin{bmatrix} A_r \\ A_\theta \\ A_\phi \end{bmatrix} = \begin{bmatrix} \sin\theta\cos\phi & \sin\theta\sin\phi & \cos\theta \\ \cos\theta\cos\phi & \cos\theta\sin\phi & -\sin\theta \\ -\sin\phi & \cos\phi & 0 \end{bmatrix} \begin{bmatrix} A_x \\ A_y \\ A_z \end{bmatrix}. \tag{21}$$

In the far field, the radial component of the electric field can be neglected compared to the θ and ϕ components. So the scattered electric field intensity is approximated by

$$E_r \approx \sqrt{E_\theta^2 + E_\phi^2}, \tag{22}$$

where E_θ and E_ϕ are defined as the following:

$$\boldsymbol{E}_\theta \approx -\frac{jke^{-jkr}}{4\pi r}\left(\boldsymbol{L}_\phi + \eta\boldsymbol{N}_\theta\right), \boldsymbol{E}_\phi \approx +\frac{jke^{-jkr}}{4\pi r}\left(\boldsymbol{L}_\theta - \eta\boldsymbol{N}_\phi\right). \tag{23}$$

Combining (19), (20) and (21), we obtain $L_\phi = L_\theta = 0$, with N_ϕ and N_θ expressed given by

$$N_\phi = -\iint_S J_x \sin\phi_r e^{jkr'\cos\psi}dx'dy', \tag{24}$$

$$N_\theta = \iint_S J_x \cos\theta_r\cos\phi_r e^{jkr'\cos\psi}dx'dy', \tag{25}$$

where $r'\cos\psi = x'\sin\theta_r\cos\phi_r + y'\sin\theta_r\sin\phi_r$.

Combining (22), (23), (24) and (25), we can obtain the ratio of the magnitude of the scattered electric field intensity to the magnitude of the incident electric field intensity:

$$\frac{E_r}{E_i} = \frac{ab}{\lambda r}\cos\theta_i \cdot Z\mathrm{sinc}(X)\mathrm{sinc}(Y), \tag{26}$$

where X, Y and Z are expressed given by

$$X = \frac{a}{\lambda}\sin\theta_r\cos\phi_r, \tag{27}$$

$$Y = \frac{b}{\lambda}(\sin\theta_r\sin\phi_r - \sin\theta_i), \tag{28}$$

$$Z = \sqrt{\sin^2\phi_r + \cos^2\theta_r\cos^2\phi_r}. \tag{29}$$

By removing the path loss $\sqrt{\frac{1}{4\pi r^2}}$, we obtain the reflection coefficient of the metal plate:

$$\beta = \sqrt{\frac{4\pi a^2 b^2}{\lambda^2}}\cos\theta_i \cdot Z\mathrm{sinc}(X)\mathrm{sinc}(Y). \tag{30}$$

Finally, we replace a and b with l and add the phase shift introduced by the IRS elements, we prove Eq. (6). □

REFERENCES

[1] T. Wang, K. Zhang, Y. Zhang, H. Tong, and C. Yin, "Near-field beam management in lis-assisted mmwave systems," in *2021 13th International Conference on Wireless Communications and Signal Processing (WCSP)*, 2021, pp. 1–6.

[2] Y. Liu, Z. Wang, J. Xu, C. Ouyang, X. Mu, and R. Schober, "Near-Field Communications: A Tutorial Review," *IEEE Open J. Commun. Soc.*, vol. 4, pp. 1999–2049, Aug. 2023.

[3] E. Björnson, Özdogan, and E. G. Larsson, "Intelligent Reflecting Surface Versus Decode-and-Forward: How Large Surfaces are Needed to Beat Relaying?" *IEEE Wireless Commun. Lett.*, vol. 9, no. 2, pp. 244–248, Feb. 2020.

[4] Q. Wu and R. Zhang, "Towards Smart and Reconfigurable Environment: Intelligent Reflecting Surface Aided Wireless Network," *IEEE Commun. Mag.*, vol. 58, no. 1, pp. 106–112, Nov. 2019.

[5] J. Sang, Y. Yuan, W. Tang, Y. Li, X. Li, S. Jin, Q. Cheng, and T. J. Cui, "Coverage Enhancement by Deploying RIS in 5G Commercial Mobile Networks: Field Trials," *IEEE Wireless Commun.*, vol. 31, no. 1, pp. 172–180, Feb. 2024.

[6] C. You, B. Zheng, W. Mei, and R. Zhang, "How to Deploy Intelligent Reflecting Surfaces in Wireless Network: BS-Side, User-Side, or Both Sides?" *J. Commun. Inf. Networks*, vol. 7, no. 1, pp. 1–10, Mar. 2022.

[7] J. Feng, B. Zheng, C. You, F. Chen, S. Zhao, W. Che, and Q. Xue, "Joint Passive Beamforming and Deployment Design for Dual Distributed-IRS Aided Communication," *IEEE Trans. Veh. Technol.*, vol. 72, no. 10, pp. 13 758–13 763, Oct. 2023.

[8] Y. Wang, Y. Zhang, Y. Ren, L. Pang, Y. Chen, and J. Li, "Joint BS-RIS-User Association and Deployment Design for Multi-RIS-Aided Wireless Networks," *IEEE Commun. Lett.*, vol. 28, no. 9, pp. 2181–2185, Sep. 2024.

[9] S. Zeng, H. Zhang, B. Di, Z. Han, and L. Song, "Reconfigurable Intelligent Surface RIS Assisted Wireless Coverage Extension: RIS Orientation and Location Optimization," *IEEE Commun. Lett.*, vol. 25, no. 1, pp. 269–273, Jan. 2021.

[10] E. Ibrahim, R. Nilsson, and J. van de Beek, "On the Position of Intelligent Reflecting Surfaces," in *Joint European Conference on Networks and Communications 6G Summit (EuCNC/6G Summit)*, Porto, Portugal, Jul. 2021.

[11] Y. Ren, R. Zhou, X. Teng, S. Meng, M. Zhou, W. Tang, X. Li, C. Li, and S. Jin, "On Deployment Position of RIS in Wireless Communication Systems: Analysis and Experimental Results," *IEEE Wireless Commun. Lett.*, vol. 12, no. 10, pp. 1756–1760, Oct. 2023.

[12] W. Tang, M. Z. Chen, X. Chen, J. Y. Dai, Y. Han, M. Di Renzo, Y. Zeng, S. Jin, Q. Cheng, and T. J. Cui, "Wireless Communications With Reconfigurable Intelligent Surface: Path Loss Modeling and Experimental Measurement," *IEEE Trans. Wireless Commun.*, vol. 20, no. 1, pp. 421–439, Jan. 2021.

[13] W. Tang, X. Chen, M. Z. Chen, J. Y. Dai, Y. Han, M. D. Renzo, S. Jin, Q. Cheng, and T. J. Cui, "Path Loss Modeling and Measurements for Reconfigurable Intelligent Surfaces in the Millimeter-Wave Frequency Band," *IEEE Trans. Commun.*, vol. 70, no. 9, pp. 6259–6276, Sep. 2022.

[14] C. Zhou, B. Lyu, C. You, and Z. Liu, "Movable Antenna Enabled Symbiotic Radio Systems: An Opportunity for Mutualism," *IEEE Wireless Commun. Lett.*, vol. 13, no. 10, pp. 2752–2756, Oct. 2024.

[15] C. A. Balanis, *Advanced Engineering Electromagnetics*, 2nd ed. Hoboken, NJ, USA: Wiley, 2012.

[16] Q. Wu, S. Zhang, B. Zheng, C. You, and R. Zhang, "Intelligent Reflecting Surface-Aided Wireless Communications: A Tutorial," *IEEE Trans. Commun.*, vol. 69, no. 5, pp. 3313–3351, May. 2021.

[17] W. Chen, X. Yang, C.-K. Wen, W. Tang, J. Wang, Y. Yuan, X. Li, and S. Jin, "Rotatable block-controlled ris: Bridging the performance gap to element-controlled systems," *IEEE Commun. Lett.*, vol. 29, no. 1, pp. 185–189, Jan. 2025.